Journal of Loremipsum 01 (2013) 1-8

JOURNAL
OF
LOREMIPSUM

www.smh.aau.dk
www.loremipsum.dk

Non-circular Chainring Optimization for Handcycling

Jonas Ø. Juhl*

Department of Health Science and Technology, Aalborg University, Fredrik Bajersvej 7, 9220 Aalborg Ø, Denmark

Accepted [Day] [Month] 2013

Abstract

This project is about optimizing the planar shape of a 52-tooth chainring for lying in phase handcycling. The angular crank velocity profile of a modeled crank-mechanism was optimized via the complex method algorithm in an inverse dynamics driven musculoskeletal model. The human model was exposed to hand forces caused by a crank torque, ensuring constant work for one revolution. Further, glenohumeral abduction profile was optimized to be certain of proper technique. Mean Cadence was set to 100 rpm.

The optimization revealed an optimized chainring shape resulting in a long duration of the transition phase furthest away from the shoulders and of the pull phase where the angular crank velocity troughs about 3.4 rad·s^{-1}. Opposite, a short duration of the transition phase closest to the shoulders and of the push phase were present, where the angular crank velocity peaks about 16.0 rad·s^{-1}.

However, an experimental crossover study, including 10 inexperienced subjects, showed a significant increase in oxygen uptake by handcycling with the non-circular chainring (1844 ml·min^{-1} ± 173 SD) compared to a circular chainring (1750 ml·min^{-1} ± 184 SD), in the last minute out of a 4-min submaximal handcycling bout at constant speed. Further, one elite handcyclist also showed a significant increase in oxygen uptake by cycling with the non-circular chainring (2189 ml·min^{-1} ± 131 SD) compared to the circular chainring (2006 ml·min^{-1} ± 179 SD) in the last 2 min out of a 6-min submaximal handcycling bout at constant speed. Therefore, the chainring design failed validation.

Keywords: Inverse dynamics simulation, Handcycling, Non-circular chainring

1. Introduction

A chainring of a handcycle is driven by the body through pedal cranks and transmits forces to the front wheel via a chain by interacting its teeth with the chain links. Conventional chainrings are, from a lateral view, circular in shape, while non-circular chainrings can be any convex shape, and thereby vary the gear ratio throughout the crank revolution. Proper design of a non-circular chainring is said to increase cycling performance by four alterations [1]:

1) Enabling the muscles to efficiently produce effective tangential forces to the pedals by a favorable angular crank velocity profile, resulting from the variable gear ratio.
2) Minimizing time spent at the low torque phases and increase time spent at the high torque phases.
3) Improve mechanical power by the change of chain lever arm throughout the crank revolution.
4) Enhance inertial load contribution to power output.

A number of different non-circular chainrings have been developed for bicycling. The first, was the Biopace oval, developed by Okijama 1983 [2], with larger radii at top and bottom dead centers and smaller radii during downstrokes, thus taking advantage of item 4. Later, contrary chainring

*Corresponding author. Tel.: +4500000000.
E-mail adress: joj08@student.aau.dk (J.Ø. Juhl)

doi:00.0000/j.jbiomech.2013.08.012

designs were developed, characterized by their smaller radii during the dead centers and larger radii during downstrokes, such as the Osymetric-Harmonic [3] and Q-Ring [4], both exploiting item 1, 2, and 3, and also preferred by today's professional road cyclists.

None of the chainring designs have proven to enhance long term cycling performance. However, the Biopace oval resulted in a significant reduction in blood lactate levels compared to a circular chainring [2] and the Q-Ring in conjunction with a rotor crank system, which rotates the cranks independently of each other to pass the dead centers more quickly, showed a higher power output in a Wingate test (11%) [4].

No non-circular chainrings have been developed for competitive handcycling, which may benefit more than bicycling, due to the "in phase" orientation of the cranks, resulting in higher relative torque fluctuation [5]. Therefore, present project optimizes a non-circular planar chainring shape, and compare the result to a similar toothed chainring, on oxygen uptake at the same travel speed, which has shown to be a good determinant of race performance [6]. The optimization process is aided by an inverse dynamics driven model, by which it is attempted to catch the complex of the musculoskeletal system, without implementing prior assumptions on which of the previous described four alterations represents the better solution, i.e., the method assesses the problem fairly objective.

2. Methods

2.1. Overview

OPTIMIZATION of angular crank velocity profile, arm kinematics, and tangential hand reaction forces, of an inverse musculoskeletal model of lying in phase handcycling, of which the mean mechanical power is constant.

MANUFACTURING of a non-circular chainring, which meets the optimized angular crank velocity best possible.

VALIDATING the performance of the optimized chainring on oxygen uptake and maximal speed, with an experiment including ten novice and one elite subject, pedaling on a handcycle ergometer.

2.2. Musculoskeletal Modeling

- Model Establishment

The inverse musculoskeletal model of handcycling was established by using the *AnyBody Modeling System v5.3.0* software [7]. The pre-established 31 segment *FreePostureHandSR* upper body model (of which 22 segments comprises the hands), from the *AnyBody Managed Model Repository v1.5*, was modified into the supine incline posture of competitive handcycling. The pelvis was attached to the initial reference system and the joint loads of the spinal column were carried by external reaction forces providing a fully supported spine.

The crank-mechanism of the handcycle was constructed of four segments. The AnyBody Modeling System does not allow custom kinematic equations, and therefore the crank was split in two interconnected segments, joined to the initial reference system to obtain the desired complexity of the angular crank velocity. A right and left handlebar segment were joined to the crank segments in phase of each other. As starting position, the cranks were oriented parallel to a line, intersecting the hub and a point midway between shoulders with the handlebars located furthest away from the shoulders.

The angular crank position θ was assigned to the crank segments with a two term sum of sine function together with a linear term and an offset, eq.1.

$$1)\quad \theta(t) = \bar{\omega}t + A_1 \cdot sin(-\bar{\omega}t + \varphi_1) + A_2 \cdot sin(-2\bar{\omega}t + \varphi_2 - Offset$$

Where $\bar{\omega}$ is the mean angular crank velocity, *t* is the time, and the *Offset* ensures that θ starts at zero to *t=0*. From a right view at the sagittal plane, the crank rotates clockwise, giving a positive θ.

The hands were joined to the handlebars with revolute joints, and therefore, moved in a circular pattern as the crank-mechanism rotated. After attaching the hands to the handlebars and forming a closed loop chain, the glenohumeral flexion and external rotation, together with elbow flexion and pronation, were unconstrained to obtain a kinematically determinate system. Glenohumeral abduction, Φ, was able to vary throughout the crank revolution by eq.2.

$$2)\quad \Phi = \Phi_0 + \Phi_{amp} sin(\theta - \tfrac{\pi}{2}) + \Phi_{amp}$$

Shoulder rhythm drivers doing clavicula protraction, -elevation, -axial rotation, and scapula protraction, and –elevation, relative to the position of humerus flexion and –elevation, were

implemented according to C.G.M. Meskers et al. [8]

A torque, τ, was inserted into the rotation center of the crank-mechanism, eq.3, causing tangential hand reaction forces.

3) $\tau(\theta) = \bar{\tau} + a_1 \cdot sin(-\theta + p_1) + a_2 \cdot sin(-2\theta + p_2)$

Where $\bar{\tau}$ is the mean torque.

About 280 simple muscles with constant strength properties spanned the shoulder-arm complex and carried the joint loads. The muscle activation pattern was estimated by minimizing a function, *G*, consisting of the sum of a quadratic and a linear term as proposed by Praagman et al. [9], eq.4.

4) $G = \sum_i (MusAct)^2 + k \sum_i MusAct$

Where *MusAct* is the relative muscle activity and *k* is a weight factor set to 0.1.

It is desired to find the optimum angular crank velocity of which the chainring shape can be derived. Therefore, the *A*'s and φ's of eq.1 are the obvious design variables, providing the model with a wide range of angular crank velocities to choose from. Also the Φ_0 and Φ_{amp} of eq.2 and the *a*'s and *p*'s of eq.3 serve as design variables to secure a proper pedaling technique, but they will have no direct effects on the optimized chainring design.

The chosen objective function to minimize, *f*, of present optimization, eq.5, has shown to perform well in predicting the torque profile in bicycling [10].

5) $f(t) = \int_0^T \sum (MusAct^2) dt$

Where *T* is the time it takes to complete one crank revolution.

T is set to *0.6 s*, and $\bar{\tau}$ is calculated as $\bar{\tau}=T \cdot 200W \cdot (2\pi)^{-1}$, leading to the cadence and mechanical power of elite handcyclists [11]. $\bar{\omega}$ is calculated as $\bar{\omega}=2\pi \cdot T^{-1}$ to ensure exactly one revolution.

Four independent optimization studies with four different initial starting values of the 10 design variables were launched using the complex method algorithm [12]. The Φ_0 and Φ_{amp} were constrained to be larger than 0.087 and 0.0 rad respectively, to avoid the elbows to penetrate the rib cage. The $min(\omega)$ was constrained to be greater than 3.4 rad·s^{-1} to ensure that it can be met by a chainring design, which fits standard spider arms of 110 mm bolt circle diameter. Otherwise, the optimization problem was unconstrained.

- *Optimization Results*

	OptS.1	OptS.2	OptS.3	OptS.4
A_1	-0.6418	0.0745	0.5953	-0.5301
φ_1	-0.3587	-0.0319	1.2124	3.8872
A_2	-0.0633	-0.2442	0.0419	-0.0016
φ_2	-.,8035	4.4296	1.9578	3.5885
a_1	13.590	10.973	-12.109	4.7697
p_1	-1.6885	-0.4479	0.5009	3.5555
a_2	-15.986	2.3411	2.5485	3.2482
p_2	-1.8159	2.1218	1.5230	1.6537
Φ_0	-0.0876	-0.0882	-0.0876	-0.0878
Φ_{amp}	0.9910	0.1044	0.9910	1.0194
Iter.	4000	3493	4000	3962
f	0.79	1.57	0.83	0.88

Tab.1: The optimized design variables of the four different optimization studies and their *f*. Initial box sizes were set as the following: *A*'s, φ's, and *p*'s are equal to 1, a's are equal to 5, and Φ's are equal to 0.14 . Population size was set to 20. The optimization studies were stopped if either the *f* or all design variables changed less than 10^{-5} over one iteration (Iter.), or if the Iter. exceeded 4000. Initial starting values were (A_1, φ_1, A_2, φ_2, a_1, p_1, a_2, p_2, Φ_0, Φ_{amp}) 1) [0, 0, 0, 0, 0, 0, 0, 0, 0, 0]; 2) [0, 1.57, 0, 4.71, 0, 1.57, 0, 4.71, 0, 0]; 3) [0.2, 0.39, 0.05, 1.57, 0, 0.39, 0, 1.57, 0, 0]; 4) [0.2, 4.71, 0.05, 4,71, 0, 3.53, 0, 4,71, 0, 0].

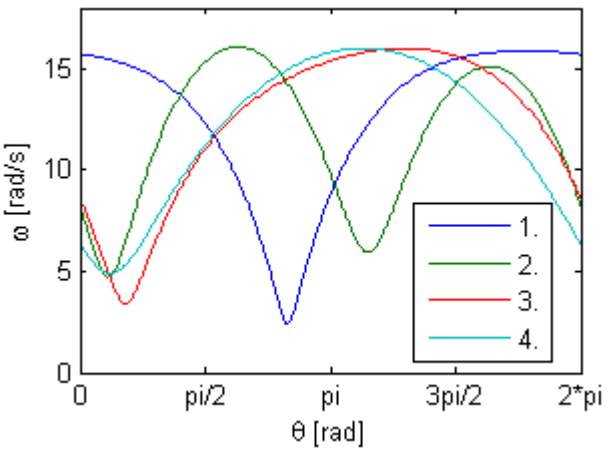

Gr.1: The four optimized ω's relative to θ.

2.3. Chainring Design

The ω profile of OptS.3 and OptS.4 share characteristics, but otherwise there are no similarities between the optimization results. OptS.1 and OptS.3 are the best solutions, and therefore, they were examined further to design the non-circular chainring.

No non-circular chainring design is able to meet the ω profile of OptS.1 or OptS.3. The problem arises because the chain wraps around the chainring, thus its larger radii will sooner or later get in the way and increase the intended chainring

radius as the chain has to wrap around these larger radii as well. Other drive-mechanisms meeting the ω profile can be applied, but will possibly lead to heavier solutions with more friction. Instead, the ω profile will be approximated best possible by a non-circular chainring, described as a radius, *r*, relative to θ. If the kinetic energy of the handcycle is large enough and the cadence is high, it can be assumed that the speed is constant throughout one crank revolution. This assumption leads to a constant chain velocity, *v* expressed as $v = \bar{r}\bar{\omega}$, and divided by the ω should give the effective chainring radius if not the chain had to wrap the chainring. Even though this approach is slightly biased, it is thought to approximate the ω well and will be included. Another problem arises with the presented approach, as the circumference will be larger than that of a circular chainring. This can simply be addressed by shifting gear to a larger sprocket. However, it is desired to keep the circumference constant, and therefore, the final expression scales down the effective chainring radius so that the circumference is constant, whatever the ω profile will be. This is done in a way, where the smallest effective radii are scaled the least and vice versa, shown by eq.6.

6) $$r = (\bar{r}\bar{\omega} \cdot \omega^{-1} - r_{min})c + r_{min}$$

Where *c* is a scaling factor, and r_{min}=0.068723 m is the lower limit of *r*, just enabling the chainring to fit standard spider arms of 110 mm bolt circle diameter. $\bar{r}$ is set to 0.105 m identical to a 52 tooth circular chainring, and *c* is set to 0.355 and 0.521 for the OptS.1 and OptS.3, respectively. The *r* for OptS.1 and OptS.3 are approximated by 52 linear pieces of 0.0127 m each, joined together at their ends to form a closed convex loop. These loops represent the interpreted planar shapes of OptS.1 and OptS.3, see fig.1.

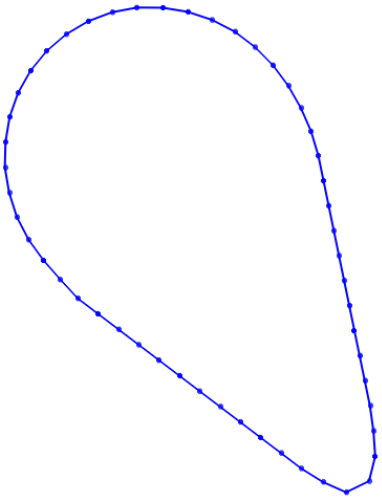

Fig.1: The interpreted OptS.3 chainring design. *r* is approximated by 52 linear pieces of 0.0127 m each, joined together at their ends to form a closed convex loop.

The f is reevaluated for both interpreted chainring designs to see if the approximation errors are negligible. Before doing this, two optimization studies were conducted on each interpreted chainring design with only the design variables of τ and Φ included, of which their initial starting values were set equal to their previous optimization result values. The A's and φ's of θ are given values to fit the real angular crank positions of the two interpreted chainring designs, see an example in gr.2 (OptS.1: A_1=0.5621, φ_1=2.1089, A_2=0.0264, φ_2=0.5262; OptS.3: A_1=0.5621, φ_1=0.9868, A_2=0.0264, φ_2=-0.5959). Otherwise, the box sizes were halved, the population set to 12, while constrains and stopping criteria remained the same.

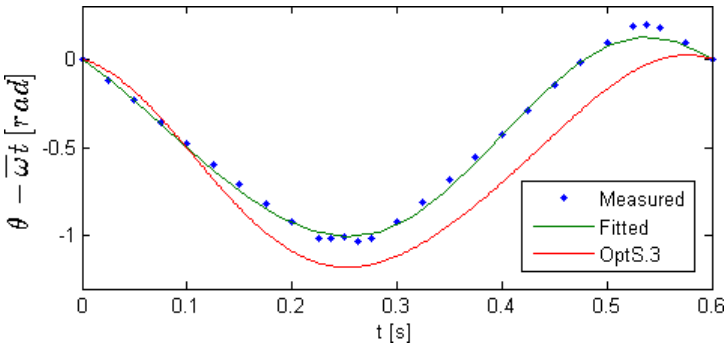

Gr.2: Showing $\theta - \bar{\omega}t$, for: measured data of the interpreted chainring of OptS.3 (blue dots), the fitted curve to measured position data (green curve), and the OptS.3 pre-interpretation (red curve). This is also done for OptS.1.

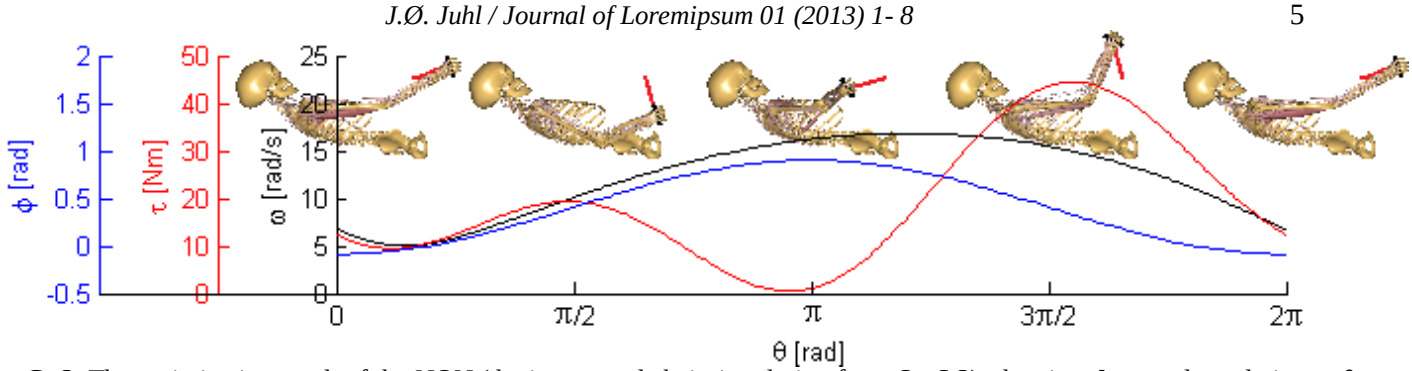

Gr.3: The optimization result of the NON (the interpreted chainring design from OptS.3), showing Φ, τ, and ω relative to θ. a_1=13.425, p_1=0.4388, a_2=-12.527, p_2=1.7393, Φ_0=-0.0875, Φ_{amp}=0.494.

The new optimization studies revealed an even better *f* of 0.73 and 0.74 for the interpreted OptS.1 and OptS.3, respectively. These *f*'s are very similar, but the interpreted OptS.3 (NON) is the chosen design as the present maximum muscle activity over one crank revolution is only 50% compared to 55% for the interpreted OptS.1. See gr.3 for the optimization results of the NON.

A chainwheel meeting the shape of the NON was produced in an universal manganese-, chromium-, tungsten- alloy tool steel, to take part in the experiment.

2.4. Validation Experiment

- Subjects

10 inexperienced male subjects (IN) participated in this study (age, height, weight, and right arm length from acromion to metacarophalangeal joint of middle finger, mean ± SD: 27.8 ± 2.2 yr; 182.8 ± 5.8 cm; 81.9 ± 9.0 kg; 68.4 ± 3.6 cm, respectively), together with an elite male subject (EL), who was a Paralympic 2012 competitor in the H3 classification (50.0 yr; 178 cm; 63 kg; 67.0 cm). The IN were not used to upper body dominated exercises, but were all active in sports. Before giving their written consent, the subjects were informed about the objective and possible risks of their participation.

- *Procedures*

A randomized crossover design was applied to investigate the effects of handcycling with the 52-tooth NON compared to a 52-tooth circular chainring (CIR). The participants tested both chainring designs at their only laboratory visit.

The subjects started out with a 10-min warm-up, with either the NON or CIR at a given speed corresponding to 100 Watt at 55 rpm with a facemask on to be accustomed to the later pulmonary gas exchange recordings. After a 2-min pause, the IN performed a 4-min bout at the same mechanical power and cadence of 100 Watt and 55 rpm, while pulmonary gas exchange was recorded. However, large variations in the degree of exertion between the IN were observed during the warm-ups, and therefore, two subjects, who felt the handcycling to be the most strenuous had their cadence and mechanical power reduced to 70 Watt at 42 rpm, and 85 Watt at 45 rpm, in their warm-up and 4-min bouts. After an 8-min pause the IN again performed a 10-min warm-up, a 2-min pause, and a 4-min bout in the same manner as before, but with the chainring swapped. Then the facemask was removed and a 2-min pause and two maximal speed bouts were performed with a 2-min pause in between. The subjects accelerated steadily to a high speed over 20 s and then pedaled all out for about 10 s until the speed decreased. An 8-min pause and a 1-min warm-up were performed before another two maximal speed bouts were done in the same manner, but with the chainring swapped.

The EL went through the same test protocol as the IN, but with the 4-min bouts prolonged to 6-min at 77 rpm and 122 W.

- *Instrumentation*

The handcycling was performed on an *Antaras A* from *Wolturnus A/S, DK-9240 Nibe,* which was mounted on a magnetic braked *Tacx Flow T2200*. The driven front wheel was loaded with an 8 kg copper cable fixed in a circle of radius 0.26 m, increasing the momentum further to get closer to real momentum of Handcycling. A 17-tooth sprocket was used to drive the front wheel. *CycleOps PowerTap G3C* powermeter was mounted to the wheel hub and the *CycleOps Joule GPS Cycling Computer 2013* was mounted on the steering device to give visual feedback of time and speed to the subjects. Cadence and mechanical power measured by the CycleOps powermeter were calibrated before each subject to 110 Watt at 60 rpm, by adjusting the resistance by the Tacx trainer software 3.12.0.

Jaeger Oxycon Pro was used to collect data from the pulmonary gas exchange and was calibrated prior to each subject.

- Experimental Validation Results

	O_2 uptake [ml·min^{-1}]		Max. speed [m·s^{-1}]	
	CIR	NON	CIR	NON
IN	1750±184	1844±173*	38.12±4.05	37.44±3.68
EL	2006±179	2189±131**	31.5	30.7

*Significant difference from the CIR (p=0.012).

**Significant difference from the CIR (p<0.001).

Tab.2: Mean oxygen uptake (±SD) for the last 60 s and 120 s, of the 4- (IN) and 6-min (EL) bouts, respectively. Mean maximal speed (±SD) for the sprint bouts. n=10 for the IN, and n=1 for the EL.

All data sets were normally tested by the Shapiro-Wilk test at the 5% significance level and showed that they were normally distributed, except for the mean speeds in the 4-min bouts for the IN, which were tested for significance with a two-tailed Wilcoxon signed rank test. All other data sets were tested for significance with a two-tailed paired-sample t-test.

No significant difference (p=0.149) was observed at the mean speed (±SD) for the IN: 5.44 ± 0.41 m·s^{-1} with the CIR and 5.40 ± 0.41 m·s^{-1} with the NON for the last 90 s. A negligible significant difference in speed was observed for the EL (p=0.02): 7.578± 0.01 m·s^{-1} with the CIR and 7.588 ± 0.01 m·s^{-1} with the NON for the last 180 s.

3. Discussion

The NON design results in a long duration of the transition phase furthest away from the shoulders and of the pull phase, where the ω troughs about 3.4 rad·s^{-1}. Opposite, a short duration of the transition phase closest to the shoulders and of the push phase was present, where the ω peaks about 16.0 rad·s^{-1}. In conjunction with the location of peak τ in the quickest phase, the design is very similar to the Biopace oval [2] and the optimization of Kautz and Hull [13], thus, its design may take advantage of enhanced inertial load contribution to power output as described in the introduction, item 4. The model is not capable of taking advantages of favorable angular crank velocity, item 1, as the implemented muscle model is too simple (more on this topic later). Improving the chainring design by minimizing time spent at the low torque phases and increase time spent at the high torque phases, item 2, does not seem to make any difference, because the work done in every phase is equal to the integration of torque over the angle. Thereby, the work done in a given phase is the same regardless of the ω profile to the same $\bar{\tau}$. Improving the mechanical power by changing the chain lever arm throughout the crank revolution, item 3, does not seem to make any difference either, due to the same reason as just outlined,. Mean mechanical power is the determining factor of cycling speed and that does not change regardless of the τ - and ω, as long as their means are constant. Considering the discussion so far, the NON design is fully understandable.

In the experiment, a lower maximal speed was obtained with the NON, even though this was not significant. This coincides with the musculoskeletal model, as the minimum muscle activity over one crank revolution is 43% for the CIR and 45% for the NON when two new optimization studies of the OptS.3 are conducted: One with unchanged ω and the other with $= \bar{\omega}$, but both with the f replaced by a function describing the most active muscle activity over one crank revolution. However, the NON failed the experimentally conducted validation by omitting the hypothesized effect of a reduced oxygen uptake in submaximal handcycling (1844 ml·min^{-1} ± 173 SD), compared to the CIR (1750 ml·min^{-1} ± 184 SD), in the last minute out of a 4-min submaximal handcycling bout at constant speed. Further, one elite handcyclists also showed an increase in oxygen uptake by cycling with the non-circular chainring (2189 ml·min^{-1} ± 131 SD), compared to the circular chainring (2006 ml·min^{-1} ± 179 SD), in the last 2 minutes out of a 6-min submaximal handcycling bout at constant speed.
The seemingly unsuccessful shape of the NON can be a result of some improper assumptions that the model is based on. The evident responsible model assumptions are: I) incorrect human model anthropometry, II) too simple muscle properties, or III) too simple modeling of the crank-mechanism.

It is difficult to detect flaws in the human model anthropometry (item I), as the model consists of 31 segments joined together with a variety of joint types, and about 280 muscles wrapping over multiple surfaces, making the model very complex. Therefore, one has to rely heavily on model stability. In some joint angles, the muscles

may suddenly wrap incorrectly about surfaces, causing an extension muscle to do flexion instead. However, it is experienced that the human model executes muscle wrappings properly with low shoulder flexion, as is the case for handcycling.

A simple muscle model describes the muscle properties of present model by assuming constant strength, regardless of the condition. This might have simplified the model too much by ignoring the force-length and force-velocity relationships of the muscles. If the force-length relationship was implemented, the optimized τ profile would probably change, as the model will be strongest in a specific range of joint angles. Also, the changed τ profile could change the ω profile, as it seems that the model prefers a high ω in high τ phases. Moreover, the implementation of the force-velocity relationship could change the ω profile, as the muscles would be stronger at a slower ω, which most probably would let the chainring design move towards slower ω's in high τ phases and vice versa. However, Rankin and Neptune did not find any influence on the shape of a bicycle chainring, by implementing the force-velocity relationship [14].

The crank-mechanism model may be too simple (item III). It does not account for the work done by the rotation of the derailleur, which only occurs with a non-circular chainring, leading to continuous storing and releasing of spring energy. If the derailleur-mechanism was implemented, the chainring design could move towards slower ω's in high τ phases and vice versa, as the spring energy is released in the push phase with the NON, reducing the muscle work in this phase and increasing it in the pull phase. Neither does the crank-mechanism account for the extra loss of energy caused by the increased vibrations, which follows with increased chainring eccentricity.

Also, the optimization problem may be too large, including too many design variables, and too much concavity in f for the complex method optimization algorithm to solve. Tab.1 shows very different results of f, indicating that it is very concave. Therefore, it is possible that better chainring designs than the NON exist. However, it was not considered to remove a sine term of the ω and τ equations (eq.1 and eq.3) to reduce the number of design variables, because the cranks are oriented in phase rather than 180^{o} "out of phase", whereby the model should have the possibility to differ between the push and pull phase.

Besides modeling flaws, the interpretation of the OptS.3 to the shape of the NON may be poor. To shed light on this, a new optimization study of the OptS.3 was conducted, but with the $\omega = \bar{\omega}$, simulating a circular chainring for comparison purposes. This optimization gave an f of 0.82, claiming that the NON, theoretically, is still a better chainring, and implying that the chainring interpretation method is good. However, this comparison of f's may be imprecise, because the ω of the NON is based on differentiation of measured position data, where small deviations leads to large fluctuations after differentation. To overcome this imprecision, the model can be improved by optimizing the chainring shape directly (instead of the ω profile), and then derive its resulting ω, whereby the interpretation step will be eliminated.

Finally, the NON may be better than CIR, but failed validation due to poor conduction of the experimental study. It can be criticized that the large IN group were all inexperienced and do not represent elite handcyclists. On the other hand, the IN had equal training with both chainrings, while it may be harder to show an improvement for the EL, who was only highly trained with the CIR. The procedure could be enhanced by letting a larger EL group complete a long-term training program including both chainrings, prior the laboratory tests. This will allow the EL to adapt to the NON, which is neccesary to benefit fully, as handcycling with the NON changes neuromuscular coordination and muscle cross sectional area requirements in specific muscles, as indicated by fig.2.

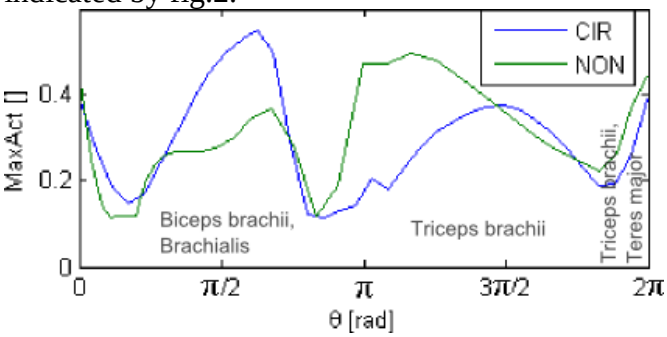

Fig.2: Theoretical maximum muscle activity present for one crank revolution for the NON and CIR. The grey text shows, which muscles are the most active in the given phase. It is seen that the NON is more demanding for the triceps brachii and less demanding for the biceps brachii, than the CIR.

Further, the kinetic energy of the flywheel and weighted wheel during the experimental tests was not big enough to match that of real handcycling. This may result in too much ω fluctuations over one crank revolution with the NON, counteracting its actual performance improvement. More inertial load or higher gearings can be altered to eliminate

this factor. Moreover, the cadence during the experimental 4- and 6-min bouts were lower than that of competitive handcycling. A lower cadence also leads to higher fluctuations in ω, counteracting the actual performance improvements of the NON. A higher cadence can be implemented to the test protocol, to smooth the ω profile, but chain dampers may be necessary, increasing frictional forces.+

As accounted for in the first section of the discussion, it is to the author's believe that the potential performance improvements with non-circular chainrings are minimal in level cycling, due to its nearly constant chain velocity. Therefore, future research is suggested to focus on theoretical chainring designs under low kinetic energy scenarios, such as uphill cycling. Then it is proposed to include the instantaneous mechanical power to the chain velocity function, to enable the model to benefit from more factors.

Acknowledgements
The author would like to thanks Wolturnus A/S for their practical support, The AnyBody Research Group, for their model support, and Supervisor Christian G. Olesen for his continual feedback.

References

[1] Rodrigo R. Bini, Frederico Dagnese. Noncircular chainrings and pedal to crank interface in cycling : a litterature review. Brazilian Journal of KINANTROPOMETRY and Human Performance, Vol 14, No 4 (2012).

[2] Ernst Albin Hansen, Kurt Jensen, Jostein Hallén, John Rasmussen, Preben K. Pedersen. *Effect of Chain Wheel Shape on Crank Torque, Freely Chosen Pedal Rate, and Physiological Responses during Submaximal Cycling*. 2009, Journal of PHYSIOLOGICAL ANTHROPO-LOGY, 28(6), 261-267.

[3] Sébastian Ratel, Pascale Duché, Christophe A. Hautier, Craig A. Williams, Mario Bedu. *Physiological responses during cycling with noncircular "Harmonic" and circular chainrings*. Eur J Appl Physiol (2004) 91: 100-104

[4] Jose A. Rodríguez-Marroyo, Juan García-Lopez, Karim Chamari, Alfredo Córdova, Olivier Hue, Jose G. Villa. *The rotor pedaling system improves anaerobic but not aerobic cycling performance in professional cyclists*. Eur J Appl Physiol (2009) 106:87-94.

[5] Paul M. Smith, Mark L. Chapman, Kathryn E. Hazlehurst, Mark A. Goss-Sampson. *The influence of crank configuration on muscle activity and torque production during arm crank ergometry*. 2008, Journal of Electromyography and Kinesiology, 18, 598-605.

[6] Thomas W. J. Janssen, Annet J. Dallmeijer, Lucas H.V. van der Woude. *Physical capacity and race performance of handcycle users*. Journal of Rehabilitation Research and Development, Vol. 38, No 1 (2001), 33-40.

[7] Michael Damsgaard, John Rasmussen, Søren Tørholm, Christensen, Egidijus Surma, Mark de Zee. *Analysis of musculoskeletal systems in the AnyBody Modeling System*. Simulation Modelling Practise and Theory, 14 (2006), 1100-1111.

[8] C.G.M. Meskers, H.M. Vermeulen, J.H. de Groot, F.C.T. van der Helm, P.M. Razing. *3D shoulder position measurements using a six-degree-of-freedom electromagnetic tracking device*. 1997, Clinical Biomechanics, 13, 280-292.

[9] M. Praagman, E.K.J. Chadwick, F.C.T. van der Helm, H.E.J. Veeger. *The relationship between two different mechanical cost functions and muscle oxygen consumption*. 2006, Journal of Biomechanics, 39, 758-765.

[10] Saeed Davoudabadi Farahani. Still unpublished: *objective functions in level and uphill bicycling, to predict crank torque.*

[11] http://www.youtube.com/watch?v=XxVjQdeKP-o. 2010, 5.8.2013

[12] Johan Andersson. *Multiobjective Optimization in Engineering Design, Applications to Fluid Power Systems*. 2001, Department of Mechanical Engineering, Institute of Technology, Linköpings Universitet.

[13] S.A. Kautz, M. L. Hull. *Dynamic optimization analysis for equipment setup problems in endurance cycling*. J. Biomechanics, Vol 28, No. 11, 1391-1401, 1995.

[14] Jeffrey W. Rankin, Richard R. Neptune. *A theoretical analysis of an optimal chainring shape to maximize crank power during isokinetic pedaling.* J. Biomechanics, 41 (2008) 1494-1502.